Physics of the Earth and Planetary Interiors 183 (2010) 404–412

Contents lists available at ScienceDirect

Physics of the Earth and Planetary Interiors

journal homepage: www.elsevier.com/locate/pepi

Equatorial paleosecular variation of the geomagnetic field from 0 to 3 Ma lavas from the Galapagos Islands

Dennis V. Kent[a,b,*], Huapei Wang[a], Pierre Rochette[c]

[a] Earth & Planetary Sciences, Rutgers University, Piscataway, NJ 08854, USA
[b] Lamont-Doherty Earth Observatory, Palisades, NY 10964, USA
[c] CEREGE, Aix-Marseille Université CNRS, 13545 Aix-en-Provence cedex 4, France

ARTICLE INFO

Article history:
Received 13 March 2010
Received in revised form 25 August 2010
Accepted 28 August 2010

Edited by: K. Zhang.

Keywords:
Paleosecular variation
Geomagnetic field
Paleomagnetism
Lavas
Pleistocene
Galapagos Islands

ABSTRACT

Complete progressive thermal demagnetization of nearly 400 oriented samples from 58 sites (lava flows) from the Galapagos Islands of Santa Cruz, San Cristobal and Floreana provide data for the statistical characterization of the time-averaged geomagnetic field near the Equator for the past few million years. Estimates of VGP dispersion due to paleosecular variation range from 9.2° to 11.8° depending on site selection criteria; our preferred estimate based on 64 site VGPs (51 accepted from this study and 13 from the 1971 study by Cox) is 11.4° (95% confidence interval 10.2–13.0°), consistent with previous estimates from the Galapagos Islands as well as paleosecular variation Model G, and confirming that angular dispersion of VGPs near the Equator is relatively low. The mean direction is not significantly different from a geocentric axial dipole field when account is taken of southward plate motion over the Galapagos hotspot. Preliminary paleointensity results from a comparison of the natural remanence with a total thermal remanence produced in a lab field of 15 μT on a subset of 321 samples from 48 sites that had relatively small changes in magnetic susceptibility after laboratory heating suggest that the time-averaged field was about 21 μT, or only two-thirds the present strength, in agreement with some other recent estimates.

1. Introduction

Secular variation is a quintessential feature of the geomagnetic field (GMF) and indicative of a geodynamo generating mechanism. Direct measurements of the GMF extend back ~400 years (Jackson et al., 2000), starting in the late 16th century at about the time of the age of exploration and widespread use of the magnetic compass, the discovery of magnetic inclination and, soon thereafter, the model of Earth as a magnet by William Gilbert in 1600 (Short, 2000). However, the quadracentennial span of the historic data is insufficiently long to capture the full scope of secular variation, which consequently requires analysis of paleomagnetic data.

Lava flows, which provide accurate readings of the GMF upon emplacement and rapid cooling, are an important source of information on secular variation over million year time scales. A key finding of paleosecular variation of recent lava (PSVRL) studies was a latitudinal variation in the dispersion of directions or their transformation into virtual geomagnetic poles (VGPs) (Cox, 1962, 1970; Creer, 1962; Creer et al., 1959; Doell and Cox, 1971; Irving and Ward, 1964; McElhinny and Merrill, 1975). PSVRL data from the equator are thus of particular importance as an end-member in the geographical dispersion spectrum. However, global analyses (e.g., McElhinny and McFadden, 1997; McFadden et al., 1988) have had to rely on very limited PSVRL data from the equatorial belt, such as the venerable study by Cox (1971) of lavas from the Galapagos Islands. New PSVRL data that meet modern reliability criteria are becoming available, for example, from Equador and Kenya (Opdyke et al., 2006, 2010); these studies tend to support relatively low VGP dispersion at the equator but questions have nevertheless been raised about the validity of any latitudinal dependence in secular variation (Johnson et al., 2008). The recommendation by McElhinny and McFadden (1997), that the PSVRL database needs to be updated, continues to be pertinent and indeed, one of the studies listed by them as worth repeating – the Galapagos lavas by Cox (1971) – is the subject of the present report.

Rochette et al. (1997) reported preliminary results from 79 sites in lavas from the Galapagos; only overall statistics were presented and the results were largely based on blanket alternating field (AF) demagnetization treatment of the samples. Given the historic importance of the Galapagos to PSVRL studies and motivated by the good possibility of obtaining high-quality data from the lavas, which were collected near sea-level and thus less likely to be affected by lightning strikes (the bane of PSVRL studies), we

* Corresponding author at: Earth & Planetary Sciences, Rutgers University, Piscataway, NJ 08854, USA.
E-mail address: dvk@rutgers.edu (D.V. Kent).

0031-9201/$ – see front matter © 2010 Elsevier B.V. All rights reserved.
doi:10.1016/j.pepi.2010.08.010

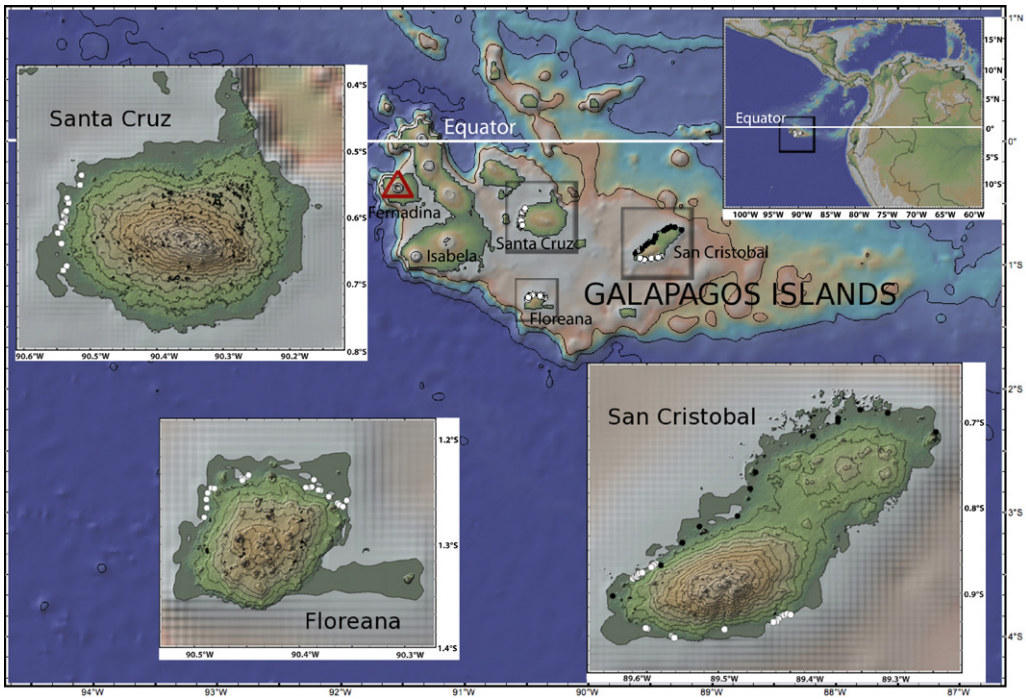

Fig. 1. Location map of sites from Galapagos Islands. The topographic maps are generated by Lamount–Doherty Earth Observatory contributed software GeoMapApp version 2.4.0 using the NASA ASTER Global Digital Elevation Model (GDEM). White circles are the sampling site locations in this study; filled circles are site locations in the study by Cox (1971).

undertook a thermal demagnetization study of 400+ specimens remaining from more than 60 sites from 3 islands in the Galapagos (San Cristobal, Santa Cruz and Floreana); these results are presented here.

2. Geology and sampling

The Galapagos Archipelago consists of volcanic islands on the Nazca plate that formed over several million years above the Galapagos hotspot, whose present eruptive center is Fernandina Island (0.37°S 91.55°W) (Fig. 1). The geology, petrology and geochemistry of the islands were described by McBirney (1994) and McBirney and Williams (1969), amongst others, and summarized by White et al. (1993) who also presented new radioisotopic age data that confirm that of the basaltic foundations of the islands extend back only a few million years (Bailey, 1976; Cox and Dalrymple, 1966; Swanson et al., 1974; see also Sinton et al., 1996).

Paleomagnetic data from Galapagos lavas were initially reported in terms of only polarities (Cox and Dalrymple, 1966) and subsequently as site-mean directions in an influential study (Cox, 1971) that constituted for many years virtually the only discrete estimate of dispersion due to PSV at the equator, even though it was based on only 17 sites from one island (San Cristobal) with hardly any demagnetization treatments. More recently, a reconnaissance study of samples collected from more than 79 sites from four of the Galapagos Islands was reported by Rochette et al. (1997); their results based on an independent set of lava sites basically agreed with Cox's estimate for dispersion due to PSV.

We report results for a subset of samples collected by Rochette et al. (1997) from sites on three Galapagos Islands: 19 sites from Santa Cruz (~0.6°S), 31 sites from San Cristobal (~0.8°S), and 24 sites from Floreana (~1.3°S) (Fig. 1). Typically eight oriented drill-core samples oriented by magnetic compass were collected at each site on shore exposures. Available geochronological data (White et al., 1993) indicate that the Galapagos Islands are younger than ~3 Ma, which would constrain the reverse and normal polarity lavas reported from these islands (Cox, 1971; Cox and Dalrymple, 1966) mainly to the Matuyama reverse chron (2.6–0.78 Ma) and Brunhes normal chron (0.78 Ma to Present).

Using the preliminary results from AF treatments to 20 mT (Rochette et al., 1997) and excluding six sites sampled on Pinzon that targeted a polarity transition, we focused on those sites which met minimum acceptance criteria (dispersion factor, $k > 50$); this excluded three sites from Santa Cruz (net 16 sites), seven sites from San Cristobal (net 24 sites), and four sites from Floreana (net 20 sites). Samples were no longer available for two additional sites (GA46 from Santa Cruz and GA61 from Floreana) that would have been otherwise acceptable, leaving a total of 58 sites (393 samples) for further analyses.

3. Paleomagnetic data

After measurement of natural remanent magnetization (NRM), a specimen from every sample was thermally demagnetized (TD) in 10–12 steps: 100 °C, (150 °C), 200 °C, (250 °C), 300 °C, 350 °C, 400 °C, 450 °C, 500 °C, 525 °C, 550 °C and 575 °C. Examples of vectors end-point demagnetization degrees are shown in Fig. 2, which show straightforward behavior characterized in most samples by linear trajectories converging to the origin after removal of minor spurious components by 300–350 °C. The unblocking temperature spectra are typically block-shaped with only a few percent of the initial NRM remaining by 575 °C, consistent with fine-grained magnetite as the main carrier of remanence. Room-temperature magnetic susceptibility measured after each demagnetization step typically showed only minor changes (Fig. 2).

The characteristic magnetization (ChRM) was estimated from each sample's demagnetization data with principal component analysis (Kirschvink, 1980) using seven steps between 350 and 575 °C. The ChRM are well defined: the average maximum angular deviation (MAD) is <1.5° and more than 95% of the sample MAD values are <5°. Grouped by site, only two sites (GA47 and GA76) had pathologically scattered directions with precision parameters <50 and were excluded. A total of 14 other samples diverged markedly (two angular standard deviations) from their site means and were

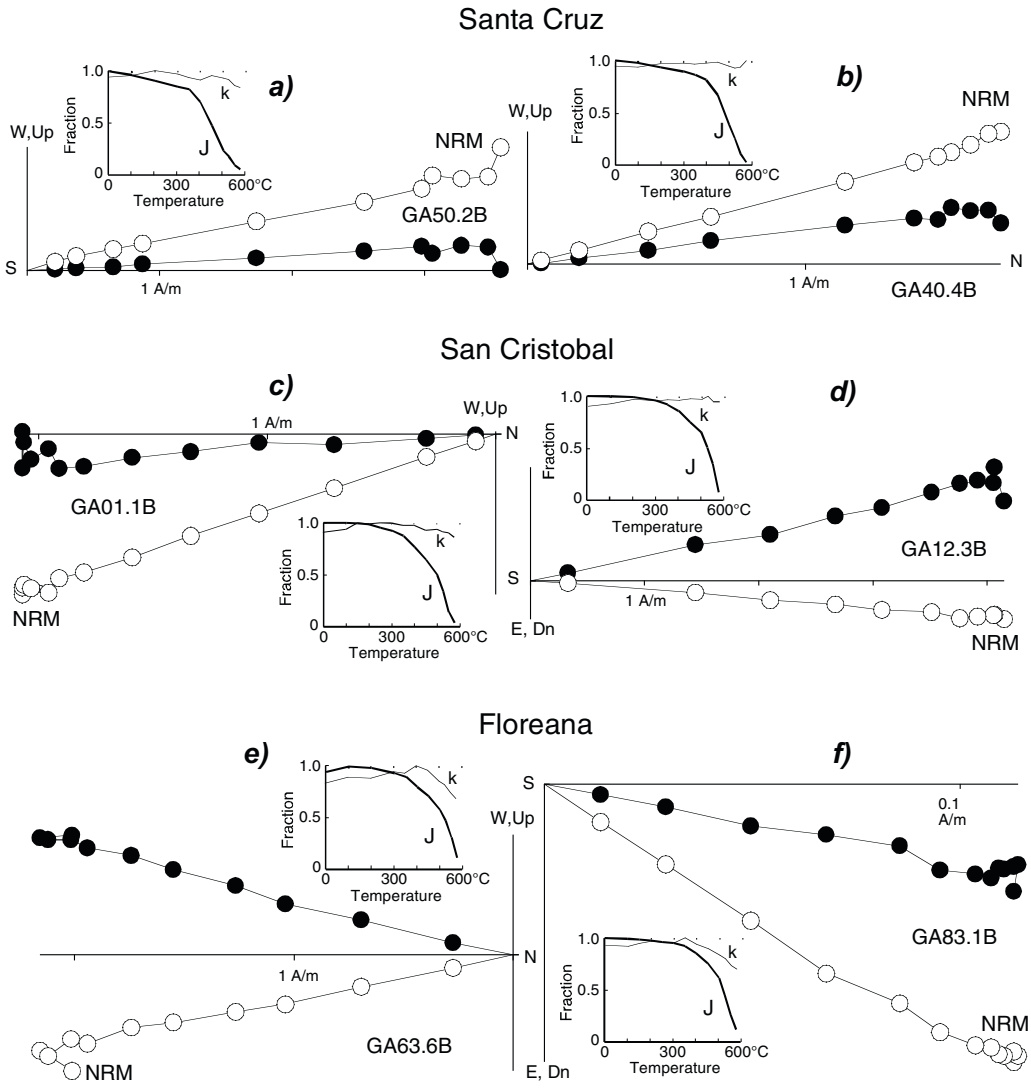

Fig. 2. Vector end-point diagrams of thermal demagnetization of NRM of representative samples of lavas from Santa Cruz (a and b), San Cristobal (c and d), and Floreana (e and f). Open (closed) symbols are projections on vertical (horizontal) planes. Thermal demagnetization steps typically were at 100 °C, 200 °C, 300 °C, 350 °C, 400 °C, 450 °C, 500 °C, 525 °C, 550 °C, and 575 °C. Insets show relative changes of sample magnetization intensity (J) and magnetic susceptibility (k) after each step.

regarded as outliers (e.g., misoriented or mislabeled) and excluded. The resulting 368 sample ChRM directions provide 54 site means with $k > 50$ (except GA28 that we chose not to exclude with $k = 47$) and a95s averaging 6° (Table 1).

The site-mean ChRM directions have a bimodal distribution: 26 sites with shallow northerly (normal polarity) directions and 28 sites with shallow southerly (reverse polarity) directions (Fig. 3a). Sites from Santa Cruz had only normal polarities whereas those from San Cristobal and Floreana had normal and reverse polarities. Four sites from Floreana (GA78, 79, 84 and 85; Table 1) give a very similar but somewhat unusual direction ($D = 212.2°$, $I = -29.8°$, a95 = 5.0°) and probably represent sampling of the same lava or closely synchronous lava flows; we combine these four site means for further analyses. The resulting 51 site data have normal and reverse polarity means with virtually identical dispersions: $D = 354.4°$, $I = 3.6°$, a95 = 5.9°, $k = 24.3$, $N = 26$ versus $D = 179.8°$, $I = -0.1°$, a95 = 5.6°, $k = 27.3$, $N = 25$. These directions are within 6.4° of antipodal and pass the reversal test at 95% confidence (classification B; McFadden and McElhinny, 1990). The overall mean direction after inverting the reverse site means is $D = 357.1°$, $I = 1.9°$, a95 = 4.1°, $k = 25.2$.

The blanket AF demagnetized data from Rochette et al. (1997) for the same sites as the TD results give very comparable results (Table 2): overall mean for the AF data ($D = 0.3°$, $I = 2.3°$, a95 = 4.1°, $k = 25.0$, $N = 51$) is within a few degrees of the TD results and the dispersions are essentially the same. Clearly these basalts have very stable magnetizations with little overprinting and respond favorably to TD or even nominal AF treatments.

The limited but independent results (5–10 mT AF for only 13 sites) from San Cristobal from Cox (1971) are shown in Fig. 3b. Only one of the 24 sites tabulated by Cox (1971) had reverse polarity but all of the 13 sites with some AF treatment had normal polarity directions. Nevertheless, the statistical measures of this dataset ($D = 358.5°$, $I = 5.2°$, a95 = 6.9°, $k = 36.7$, $N = 13$; Table 2) are not significantly different from either the AF results (Rochette et al., 1997) or the TD results reported here for 51 sites from Santa Cruz, Floreana, as well as San Cristobal. Each of these datasets apparently captured a sufficient time span in rocks with stable magnetizations to yield comparable estimates of the time-averaged GMF.

4. Paleosecular variation estimate

VGPs calculated from the ChRM site means and site locations are well grouped around a mean paleopole located at 86.5°N 217.3°E A95 = 3.0°, $K = 44.8$, $N = 51$ (Fig. 3c). The paleopole is slightly (but significantly) near-sided with respect to the geographic axis; we

Table 1
Site mean locations, stable magnetic directions and VGPs for sampling sites from San Cristobal, Santa Cruz and Floreana in Galapagos Archipelago.

Site	sLat (°)	sLon (°)	*n*	*R*	*k*	a95 (°)	Dec (°)	Inc (°)	vgpLO (°)	vgpLA (°)
San Cristobal (TD data)										
GA01	−0.92667	−89.42633	7	6.9476	114.6	5.7	181.9	17.9	257.7	−81.5
GA02	−0.92667	−89.42633	5	4.9934	604.9	3.1	177.1	22.2	285.6	−79.0
GA03	−0.92533	−89.42350	7	6.9437	106.7	5.9	354.0	−7.4	155.5	83.4
GA05	−0.92533	−89.42350	5	4.9264	54.3	10.5	340.3	−.9	181.8	70.3
GA06	−0.92383	−89.42000	8	7.9092	77.1	6.3	352.0	3.4	198.7	81.6
GA09	−0.92483	−89.41600	7	6.9726	219.1	4.1	343.6	−3.2	178.1	73.6
GA10	−0.92983	−89.43017	4	3.9408	50.7	13.0	175.7	3.2	351.6	−85.6
GA11	−0.93267	−89.43250	6	5.9582	119.7	6.1	354.4	−4.4	167.7	84.3
GA12	−0.93333	−89.43600	6	5.9717	176.8	5.1	344.0	2.4	188.1	73.9
GA15	−0.94183	−89.49300	6	5.9771	218.0	4.5	182.9	5.6	213.3	−86.6
GA18	−0.94950	−89.55417	7	6.9172	72.5	7.1	181.2	.7	153	−88.7
GA19	−0.95100	−89.55250	7	6.9594	147.6	5.0	178.3	5.1	317.1	−87.7
GA20	−0.95167	−89.55133	6	5.9843	317.7	3.8	185.0	10.4	221.2	−83.4
GA21	−0.94100	−89.58283	5	4.9845	257.4	4.8	185.0	−3.9	150.4	−84.2
GA22	−0.94033	−89.58466	6	5.9402	83.6	7.4	179.0	9.5	285.0	−86.0
GA23	−0.88267	−89.59950	7	6.9064	64.1	7.6	162.5	3.2	357.9	−72.5
GA24	−0.88267	−89.59950	7	6.9753	242.8	3.9	167.1	1.3	1.3	−77.1
GA25	−0.88033	−89.59700	8	7.9555	157.3	4.4	179.3	−1.9	69.5	−88.0
GA26	−0.88033	−89.59500	8	7.9562	159.8	4.4	166.3	13.1	337.2	−75.2
GA27	−0.87800	−89.59400	8	7.9689	224.8	3.7	186.2	−3.0	159.4	−83.4
GA28	−0.87667	−89.59200	5	4.9146	46.8	11.3	179.7	−2.9	83.1	−87.7
GA29	−0.87583	−89.58850	5	4.9734	150.1	6.3	184.2	−40.7	99.8	−65.5
GA30	−0.86550	−89.57300	8	7.9408	118.2	5.1	356.3	−4.9	157.1	86.0
GA31	−0.86717	−89.57550	8	7.9044	73.3	6.5	358.8	−9.5	107.4	85.9
Santa Cruz (TD data)										
GA33	−0.60117	−90.53934	8	7.9279	97.1	5.7	345.7	−.5	180.8	75.7
GA34	−0.59950	−90.53967	7	6.9710	207.2	4.2	346.1	2.8	187.7	76.0
GA35	−0.59683	−90.53983	8	7.9728	257.1	3.5	346.2	3.6	189.3	76.0
xGA38	−0.60683	−90.53833	8	7.8916	64.6	6.9	333.6	22.3	205.2	61.1
xGA39	−0.60800	−90.54134	8	7.9352	108.0	5.4	18.5	45.1	301.3	57.4
GA40	−0.60967	−90.54200	7	6.9678	186.6	4.4	351.2	−13.0	145.0	79.4
GA44	−0.59150	−90.53767	9	8.9442	143.5	4.3	352.4	−1.1	179.7	82.4
GA45	−0.59033	−90.53584	7	6.9568	139.0	5.1	350.1	−.4	181.7	80.1
GA47	−0.57083	−90.53484	5	4.4360	7.1	30.9	346.4	9.3		
GA48	−0.57083	−90.53484	5	4.9974	1512.9	2.0	354.4	23.5	246.2	76.0
GA49	−0.55117	−90.51534	7	6.9821	335.5	3.3	359.0	−4.4	120.7	88.1
GA50	−0.53667	−90.51317	8	7.9688	224.2	3.7	358.7	−9.3	106.9	85.7
GA58	−0.67983	−90.54050	6	5.9662	148.0	5.5	6.7	3.2	340.7	82.9
GA59	−0.67333	−90.53550	7	6.9633	163.7	4.7	1.8	1.5	321.1	87.7
Floreana (TD data)										
GA60	−1.26083	−90.36383	6	5.9263	67.8	8.2	351.7	12.9	223.0	78.6
GA63	−1.25833	−90.35516	8	7.9322	103.3	5.5	187.2	4.4	187.2	−82.7
GA64	−1.25517	−90.37200	7	6.9692	194.8	4.3	180.5	1.3	129.2	−89.2
GA65	−1.25450	−90.37217	8	7.8664	52.4	7.7	172.3	2.0	1.4	−82.3
GA66	−1.24867	−90.37984	7	6.9829	351.4	3.2	185.0	−.6	162.4	−84.8
GA67	−1.24817	−90.38200	5	4.9603	100.8	7.7	180.2	−.3	97.8	−88.6
GA69	−1.24600	−90.39267	5	4.9280	55.5	10.4	1.7	4.6	295.2	86.1
GA70	−1.23867	−90.38633	6	5.9827	289.2	3.9	177.9	−13.3	74.9	−81.7
GA71	−1.23867	−90.38633	7	6.9645	169.1	4.7	176.0	−9.8	56.7	−82.6
GA72	−1.24600	−90.39400	6	5.9441	89.5	7.1	4.9	5.1	321.8	83.8
GA74	−1.23417	−90.44833	7	6.9771	262.0	3.7	8.9	−7.2	14.7	80.8
GA76	−1.23817	−90.45333	4	3.9257	40.4	14.6	351.5	39.5		
*GA78	−1.24650	−90.48383	8	7.9693	228.4	3.7	212.2	−29.8	149.8	−53.8
*GA79	−1.25117	−90.48717	7	6.9189	74.0	7.1	210.0	−28.6	149.3	−56.1
GA82	−1.27433	−90.49050	7	6.9084	65.5	7.5	177.6	−3.4	50.6	−86.2
GA83	−1.27433	−90.49050	8	7.9486	136.1	4.8	7.9	32.8	291.3	69.3
*GA84	−1.27433	−90.49050	8	7.9349	107.6	5.4	217.1	−25.0	156.9	−50.5
*GA85	−1.25733	−90.48850	7	6.9773	264.3	3.7	211.5	−22.4	156.2	−56.1
xGA78–85	−1.25730	−90.48800	4	3.9913	344.6	5.0	212.7	−26.5	153.1	−54.2
San Cristobal (AF data from Table 1 in Cox (1971))										
G104	−0.778	270.537	8	10.9194	655	2.2	349.0	21.2	227.8	74.0
G102	−0.810	270.522	8	3.9898	792	2.0	359.7	−17.2	92.6	82.0
G112	−0.686	270.665	8	8.9775	1260	1.6	014.1	7.4	343.2	75.2
G100	−0.822	270.478	8	2.9835	416	2.7	003.3	11.4	296.8	82.7
G107	−0.717	270.610	8	2.9941	1379	1.5	354.8	9.0	225.7	82.6
G113	−0.690	270.697	8	3.9731	387	2.8	358.4	8.8	253.6	84.6
G110	−0.700	270.639	8	2.9974	703	2.1	005.0	4.5	329.9	84.2
G111	−0.696	270.639	8	3.9919	871	1.9	005.0	6.8	321.1	83.6
G116	−0.712	270.753	8	2.9930	996	1.8	338.1	13.4	200.0	66.9
G118	−0.759	270.543	8	3.9871	993	1.8	352.7	−11.2	146.3	81.2
G098	−0.841	270.458	8	2.9941	1295	1.5	358.0	6.6	224.8	85.4
G096	−0.867	270.433	8	3.9922	617	2.2	359.2	−3.7	129.6	88.8
G122	−0.903	270.377	8	3.9816	744	2.0	001.9	9.6	288.7	84.0

sLat and sLon are the latitudes and longitudes for the sampling sites. *n* is the number of samples that provided acceptable data from a site, *R* is the resultant of their unit vector length, *k* is the best estimate of Fisher's precision parameter, a95 is the radius of the 95% confidence circle around the site mean direction in terms of declination, Dec, and inclination, Inc. The corresponding virtual geomagnetic pole is located at vgpLO, the longitude, and vgpLA, the latitude. The sites marked by * were averaged to a single mean labeled GA78-85; the sites marked with x would be excluded from overall averages on basis of VGP exceeding a cutoff angle according to method of Vandamme (1994); sites GA47 and GA76 were rejected due to poor within-site grouping.

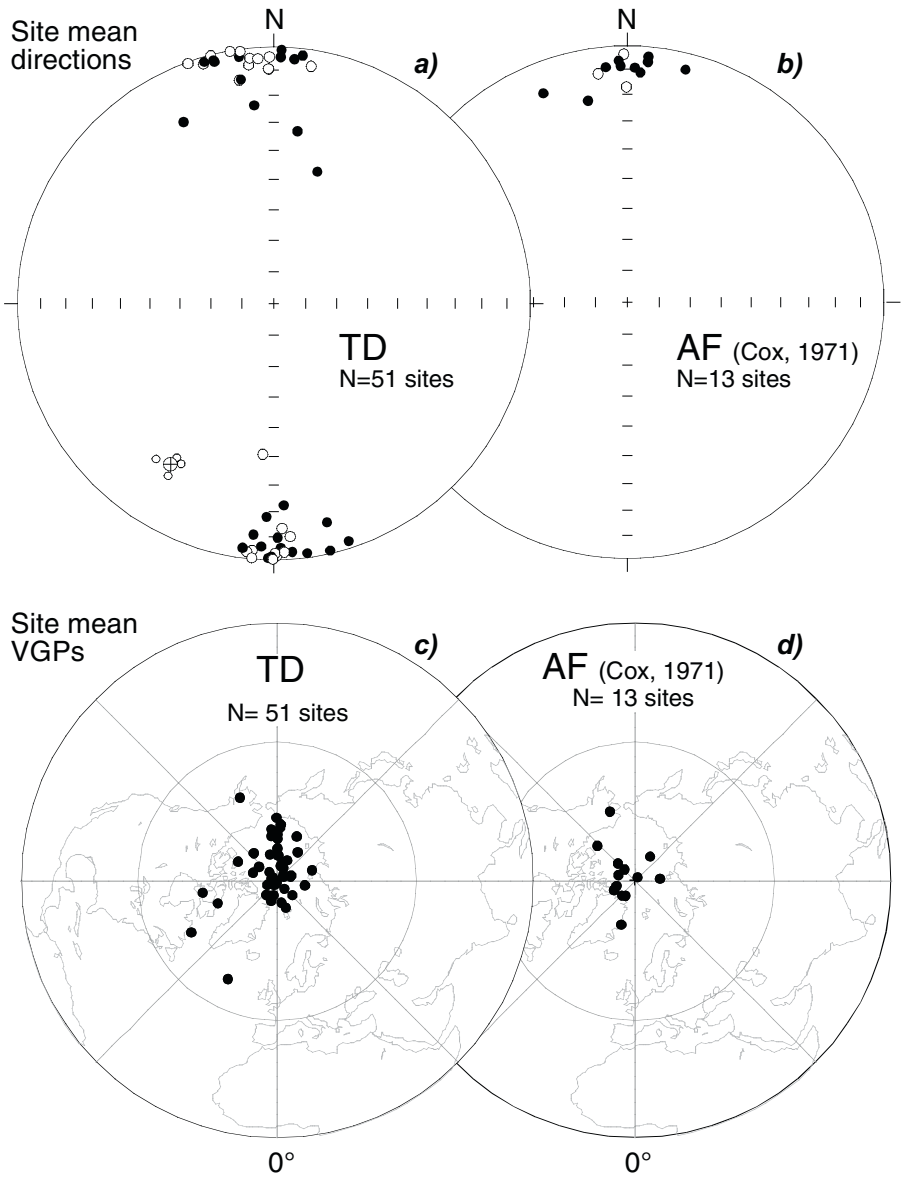

Fig. 3. Site-mean directions for Galapagos lavas based on (a) most stable component isolated with thermal demagnetization (TD) or (b) alternating field demagnetization (AF; data from Cox (1971)). Open (closed) symbols plotted on lower (upper) hemispheres of equal-area projections. Larger open circle with cross is the mean of four sites (GA78, 79, 84, 85) with nearly the same direction (see Table 1). Corresponding site VGPs for Galapagos lavas are plotted in common (normal) polarity for (c) thermal demagnetization (TD) data and (d) alternating field (AF) data from Cox (1971); statistics for 64 site VGPs are mean pole: 222.9°E 86.5°N (A95 = 2.6°); dispersion, S_b = 11.4° (confidence interval = 10.2–13.0°): elongation, E = 2.08 (confidence interval = 1.27–3.95), which is consistent with model TK03 (L. Tauxe, 2010 personal communication).

will return to this point in Section 7. Three site VGPs depart from the mean paleopole somewhat more than a cutoff angle of 25.5° obtained by the method of Vandamme (1994); we chose to retain these sites but include statistics for the filtered dataset in Table 2 for reference.

The independent dataset of VGPs from the AF sites from Cox (1971) (Fig. 3d) can be combined with the TD dataset to improve the overall basis for statistical inference. The combined dataset of 64 site VGPs gives an overall mean paleopole at 86.5°N 222.9°E A95 = 2.6°, K = 48, which is also slightly but significantly near-sided.

We use standard procedures to estimate angular dispersion of the GMF from the distribution of site VGPs (e.g., McElhinny and Merrill, 1975). The angular standard deviation, S, is estimated as:

$$S = \frac{81}{sqrt(K)}$$

where K is Fisher's concentration factor:

$$K = \frac{N-1}{N-R}$$

where R is the resultant vector length of N unit (site VGP) vectors.

The total dispersion (S_t) is a combination of the scatter caused by GMF variations from site to site (S_b) and the within-site scatter (S_w) due to measurement and recording errors:

$$S_t^2 = \frac{S_b^2 + S_w^2}{n}$$

where n is the average number of samples used per site.

Estimates of S_b are summarized in Table 2 for various combinations of datasets and selection criteria. A relatively conservative estimate is 11.8° (95% confidence interval 10.4–13.7°) for the 51 TD sites, which is practically the same as 11.7° for the same 51 sites using AF demagnetization and 11.2° for 66 AF demagnetized sites after filtering with an optimal cutoff angle of 26.2° (Rochette et al.,

Table 2
Estimates of VGP dispersion for Galapagos lavas datasets.

ID	DMG	*N*	*k*	a95 (°)	DEC (°)	INC (°)	VGP						
							K	A95 (°)	LON (°)	LAT (°)	S_b (°)	lS_b (°)	uS_b (°)
A	TD	51	25.2	4.1	357.1	1.9	44.8	3.0	217.3	86.5	11.8	10.4	13.7
B	AF	51	25.0	4.1	0.3	2.3	46.0	3.0	280.9	87.6	11.7	10.3	13.6
C	TD	48	37.9	3.4	356.6	0.1	72.6	2.4	198.2	86.4	9.2	8.1	10.7
D	AF	66									11.2	9.9	12.9
E	AF	13	36.7	6.9	358.5	5.2	63.9	5.2	253.9	86.3	10.1	8.0	13.8
F	NRM	17	33.0	6.4	358.8	2.5	54.0	4.9	239.3	87.6	10.9	9.1	14.8
A + E	TD + AF	64	27.0	3.5	357.4	2.6	48.2	2.6	222.9	86.5	11.4	10.2	13.0
C + E	TD + AF	61	37.2	3.0	357.0	1.2	70.8	2.2	207.8	86.6	9.5	8.5	10.8

Various dispersion estimates for datasets are identified in column ID (see below); DMG is treatment (TD, thermally demagnetized; AF, alternating field; NRM is natural remanent magnetization with no TD or AF treatment); *N* is number of sites, *k* is Fisher's precision parameter and a95 is radius of circle of confidence around mean declination, DEC, and inclination, INC, whereas *K* and A95 are corresponding precision parameter and circle of confidence for mean longitude, LON, and latitude, LAT, of site VGPs. S_b is between-site dispersion of VGPs with respect to mean pole position and corrected for within-site dispersion, with lower (lS_b) and upper (uS_b) bounds of 95% confidence interval using method of Cox (1969). In column ID, A: TD sites with $k > 50$ and combining GA78, 79, 84 and 85 (this paper). B: same sites as A using blanket AF, $k > 50$ (Rochette et al., 1997). C: same as A with cutoff angle of 25.5°. D: blanket AF, $k > 20$, and cutoff angle of 26.3° (Rochette et al., 1997). E: AF sites from Cox (1971). F: mainly NRM sites filtered to remove redundancies, providing the dispersion value often quoted for the Galapagos (Cox, 1971). A + E: combined TD and Cox AF sites as our preferred estimate (in bold). C + E: combined TD and Cox AF sites with cutoff angle of 25.5°.

1997). If the same filtering method of Vandamme (1994) is used on the 51 TD sites, the optimal cutoff angle of 25.5° reduces the number of sites to 48 and results in a corrected between-site dispersion of 9.2° (confidence interval 8.1–10.7°). The choice of cutoff angle is clearly important (McElhinny and Merrill, 1975). The 48 filtered TD and 13 Cox AF sites are independent and can be combined to yield an estimate of 9.5° (confidence interval 8.5–10.8°) for angular dispersion. Without a cutoff, the combined 64 sites (51 TD plus 13 Cox AF) would yield an angular dispersion of 11.4° (confidence interval 10.2–13.0°).

5. Comparison to other dispersion estimates

The between-site VGP dispersion for the Galapagos lavas most probably (95% confidence) lies somewhere between 8.1 and 13.8 °C, depending on which subset of acceptable data is selected from the 51 TD sites from Santa Cruz, San Cristobal and Floreana and 13 AF sites from San Cristobal from Cox (1971). This range is consistent with previous estimates for VGP dispersion from Galapagos lavas (Cox, 1971; Rochette et al., 1997) but it is now based on fully demagnetized and tabulated data. The chances of redundancy are reduced since the TD dataset comes from three different islands (i.e., volcanic centers) and independent laboratory studies. The correct value of dispersion may very well be at the lower end of the estimated range but a representative estimate is 11.4° (confidence interval 10.2–13.0°) based on 51 TD sites reported here and 13 AF sites from Cox (1971) without a cutoff.

The VGP angular dispersion from Galapagos lavas compares well with some recent estimates from other near-equatorial PSVRL studies (Fig. 4 and Table 3), notably Mt. Kenya at 0° latitude (S_b = 11.0°, confidence interval 9.2–12.7°) and Loiyangalani at 2.6°N (S_b = 9.3°, confidence interval 7.9–11.1°) (Opdyke et al., 2010). However, the angular dispersion for Equador at 0.6°S (S_b = 14.0°, confidence

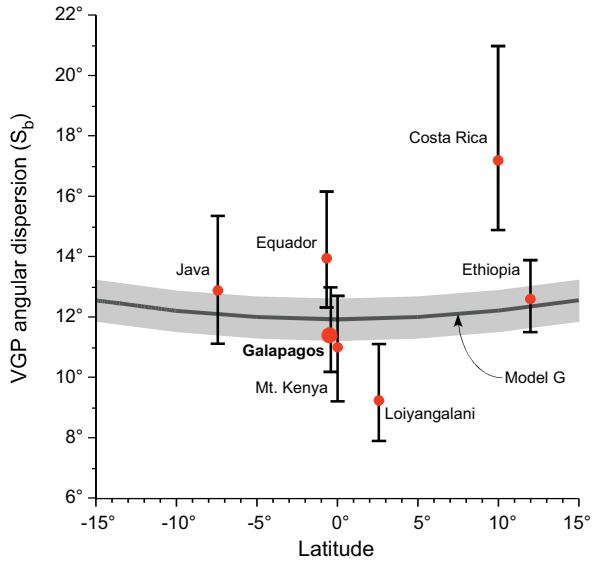

Fig. 4. VGP angular dispersion (S_b, with lower and upper 95% confidence limits) for Galapagos lavas compared to other estimates within 15° of the Equator (see Table 3 for references). Curve is latitudinal variation of S_b (with 95% confidence envelope) of latitudinally-binned PSVRL data fitted to Model G (McElhinny and McFadden, 1997).

Table 3
Estimates of VGP angular dispersion within 15° of the equator.

Locality	sLat (°)	sLon (°)	*N*	S_b (°)	lS_b (°)	uS_b (°)	Reference
Java	−7.4	112.0	35	12.9	11.1	15.4	Elmaleh et al. (2004)
Equador	−0.6	51.0	51	14.0	12.3	16.2	Opdyke et al. (2006)
Galapagos	−0.4	268.4	64	11.4	10.2	13.0	This paper
Mt Kenya	0.0	36.5	69	11.0	9.2	12.7	Opdyke et al. (2010)
Loiyangalani	2.6	36.5	32	9.3	7.9	11.1	
Costa Rica	10.0	276.0	28	17.2	14.9	21.0	Constable et al. in Johnson et al. (2008)
Ethiopia	12.0	41.5	103	12.6	11.5	13.9	Kidane et al. (2003)
Binned 0–4.9°	2.1		138	11.1	10.2	12.1	McElhinny and McFadden (1997)
Binned 5–14.9°	11.5		113	12.3	11.2	13.6	

sLat is the nominal latitude and sLon the longitude of the sampling localities, *N* is the number of lava sites, S_b is between-site dispersion of VGPs with respect to mean pole position and corrected for within-site dispersion, with lower (lS_b) and upper (uS_b) bounds of 95% confidence interval using method of Cox (1969). Binned entries were averaged in latitudinal bands from both hemispheres and are from Table 4b in McElhinny and McFadden (1997).

interval 12.3–16.2°; Opdyke et al., 2006) is several degrees higher than these estimates; we suspect this is because of jitter from undetected tilting of lavas in that active Andean tectonic setting. According to a compilation by Opdyke et al. (2010), the only other datasets within 15° of the equator that meet modern reliability standards are from Java at 7.4°S (S_b = 12.9°, confidence interval 11.0–15.4°; Elmaleh et al., 2004), Costa Rica at 10°N (S_b = 17.2°, confidence interval 14.9–21.0°; Johnson et al., 2008), and the Afar region of Ethiopia at 12°N (S_b = 12.6°, confidence interval 11.5–13.9°; Kidane et al., 2003). The Costa Rica dispersion estimate seems anomalously high, which as suspected for Equador might also reflect a contribution from undetected tectonic tilts of the lava flows. In contrast, the more quiescent tectonic setting of the Galapagos may have reduced this potential source of recorder noise.

To compensate for the small size of individual datasets and improve temporal sampling, lava data have also been binned into latitude bands (McElhinny and Merrill, 1975). In an important and widely used compilation of 0–5 Ma lava data, McElhinny and McFadden (1997) estimated a VGP dispersion of 11.1° (95% confidence interval 10.2–12.1°) for 138 sampling sites within 5° of the equator (average latitude 2.1°) that passed reasonably stringent selection criteria (all samples demagnetized, site a95 <10°, more than 2 samples per site). The new dispersion estimates from Kenya (Opdyke et al., 2010) and the Galapagos (this paper) are in good agreement with this binned estimate, which together reinforce the notion that VGP dispersion at the equator over the past few million years was in fact low compared to higher latitudes.

6. Preliminary time-averaged paleointensity

The excellent directional results from thermal demagnetization of NRM suggested that the Galapagos lavas may also be good recorders of geomagnetic field intensity. Reconnaissance rock magnetic studies on about two dozen samples also indicated favorable properties: susceptibility versus temperature curves are often nearly reversible with Curie points predominantly around 575 °C consistent with magnetite whereas hysteresis parameters (Day et al., 1977) indicate that the remanence carriers tend to be fine-grained (Mr/Ms ~0.1–0.4, mean ~0.20) (Fig. 5). These magnetic characteristics are similar to those reported for other subaerial basalts such as from Hawaii (e.g., Herrero-Bervera and Valet, 2009) and Kenya (Opdyke et al., 2010). In anticipation of mounting a full-fledged Thellier paleointensity campaign with more detailed rock magnetic investigations, we compared the NRM vector that was unblocked between 350°C (sufficient to exclude viscous components) and 575 °C (close to the maximum unblocking temperature) to a corresponding laboratory thermoremanence (TRM) produced by heating the sample to 575 °C, cooling it to room temperature in a field of 15 μT, and thermally demagnetizing the resultant TRM at 350 °C. Measurements of room-temperature magnetic susceptibility were made after each heating to monitor laboratory-induced thermomagnetic alteration; after 575 °C, most of the samples had susceptibility changes of less that 50% compared to initial values, which we used as a criteria for rejecting about 10% of the samples with greater changes.

Ideally, the ratio of NRM to TRM multiplied by the laboratory field (15 μT), which we refer to as *Pint*, should be a measure of the ancient GMF intensity in which the sample acquired the stable fraction of its NRM during initial cooling. Although our data were produced using the underlying principles of the classic Thellier–Thellier paleointensity experiment (Thellier and Thellier, 1959) and its variants (e.g., Coe, 1967; Aitken et al., 1988; Tauxe and Staudigel, 2004), which include numerous and elaborate internal checks for reliability, our procedure is intended to provide only a rough estimate of the paleointensity distribution, relying on a modest criteria for laboratory-induced alteration (susceptibility changes) and statistical coherence in both directions and paleointensities at the within-site level. The main virtue of our experimental strategy is that a large population of samples that

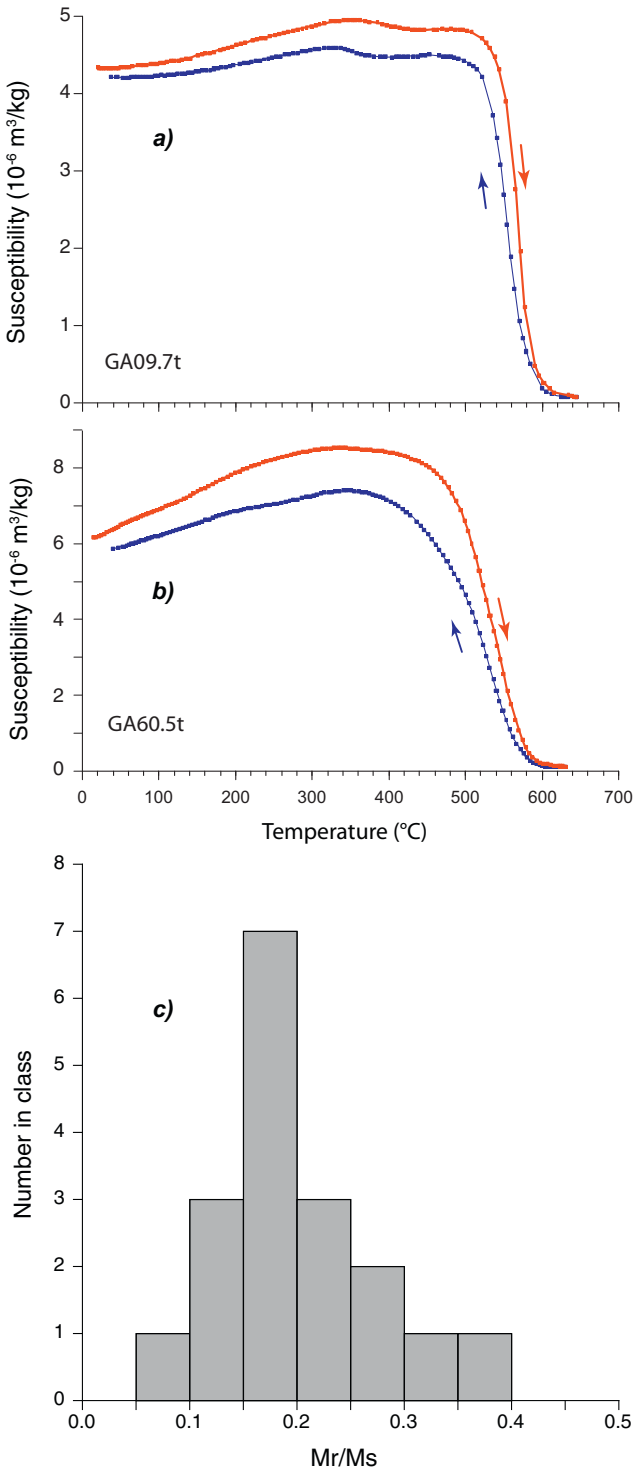

Fig. 5. (a and b) Magnetic susceptibility versus temperature for two basalt samples from the Galapagos Islands; heating and cooling curves are indicated by arrows. Sample Ga09.7t (a) is from site with *Pint* estimate of 57.4 μT; sample Ga60.5t (b) is from site with *Pint* estimate of 7.2 μT. (c) Histogram of Mr/Ms values from 18 basalt samples from the Galapagos Islands. Hysteresis measurements were made in up to a 1 T direct field on a Princeton Measurements VSM Model 2900.

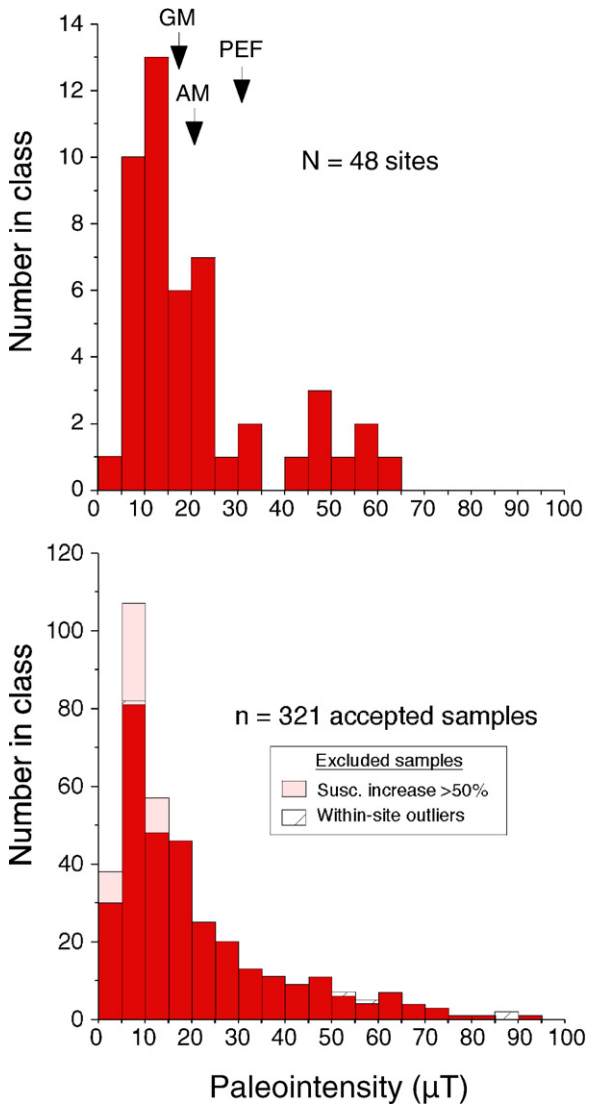

Fig. 6. Estimates of paleointensity for 321 samples (bottom histogram) based on ratio of stable component of NRM (350–575 °C) to TRM produced by cooling from 575 °C in laboratory field of 15 μT and thermally demagnetized to 350 °C. Histogram in top panel shows distribution of site mean paleointensity estimates compared to strength of present Earth's field (PEF); GM is geometric mean and AM is arithmetic mean for the 48 site values.

had been thermally demagnetized can be quickly processed for paleointensity and the prospects of success for full Thellier experiments assessed at a site-by-site level. Another mitigating benefit of using a total TRM method is that it minimizes nonlinear effects from multidomain contributions (e.g., see Fig. 49 in Dunlop and Ozdemir (2007)).

In the case of the Galapagos lavas, the mean *Pint* value for 321 accepted samples is 20.8 μT; grouped and averaged by site (after excluding as within-site outliers a handful of samples with values more than twice the standard deviation away from the initial site mean), the overall mean *Pint* value for 48 sites, which best represents the time-averaged field intensity, was practically the same (21.0 μT) since the number of samples per site is similar (Fig. 6). The sample or site-mean *Pint* values have a tail toward higher values and may be better represented by a log-normal distribution; the corresponding geometric mean value for the 48 sites is 17 μT. In comparison, the field intensity in the Galapagos today is ~30 μT.

7. Discussion

In their compilation of 0–5 Ma lava data, McElhinny and McFadden (1997) found an overall latitudinal variation of VGP dispersion that was fit to Model G (McFadden et al., 1988) with a zero-latitude (equatorial) value of 11.9 ± 0.7° (Fig. 4), which was used, for example, to constrain GMF statistical model TK03 (Tauxe and Kent, 2004). In contrast, Johnson et al. (2008) suggested that the available PSVRL data made it difficult to discriminate between PSV models that predict virtually no VGP dispersion with latitude (e.g., Constable and Parker, 1988) from those with a latitudinal increase in S_b (e.g., McElhinny and McFadden, 1997; Tauxe and Kent, 2004). However, the new equatorial results from lavas in Kenya (Opdyke et al., 2010) and the Galapagos (this paper) and recent results from ~78°S in Antarctica (Lawrence et al., 2009) are consistent with a significant increase in VGP dispersion by around a factor of two from equatorial (S_b ~11°) to polar (S_b ~24°) latitudes, as suggested by Model G of McElhinny and McFadden (1997).

The time-averaged mean direction or pole position in the Galapagos dataset departs by a few degrees from that of a geocentric axial dipole, which for the mean site latitude of 0.95°S would predict a mean normal polarity inclination of −1.9°. Instead, the mean inclination (TD + AF Cox dataset with reverse sites inverted) is 2.6 ± 3.5°, which is just significantly different as is the mean VGP (86.5 ± 2.6° latitude) from the geographic axis (Table 2). One interpretation is that the departure is evidence of a few percent contribution from an axial quadrupole field; however, since the mean VGP is near-sided and the inclination anomaly is positive, this would imply the time-averaged quadrupole contribution would have to be of opposite sign to most previous estimates (e.g., Johnson et al., 2008; Wilson, 1971). Alternatively, once formed over the hotspot the Galapagos Islands on the Nazca plate have been moving south and this needs to be taken into account. Assuming that the hotspot has remained relatively fixed at the present locus of hotspot activity at 0.37°S (Fernandina Island), the sampling sites have moved nearly 0.6° in latitude; in other words, the predicted inclination would be −0.7°. This would be sufficient to account for much of the apparent departure and make the mean directions indistinguishable (95% confidence level) from that of a geocentric axial dipole field.

Lastly, a rudimentary total TRM paleointensity procedure that takes advantage of the thermal demagnetization of NRM data provides coherent results from 321 samples from 48 sites. The mean value of the distribution suggests that the intensity of the time-averaged GMF at the equator was only about 21 μT, or roughly the two-thirds the present-day value at the Galapagos locality (~30 μT). It is entirely possible that the lavas have increased their ability to acquire TRM when they alter during laboratory heating, which would result in underestimates of paleointensity, although using a somewhat more stringent acceptance criteria does not seem to markedly change the mean paleointensity value (e.g., 21.3 μT for 286 accepted samples for <20% susceptibility change compared to 20.8 μT for 321 accepted samples for <50% susceptibility change). Compilations of paleointensity data for the past few million years have tended to produce average values that are close to the present-day field although there is some suspicion the data distribution may not adequately reflect paleointensity variations at the million-year time scale (Selkin and Tauxe, 2000). The Galapagos total TRM results obviously need to be confirmed by full Thellier experiments with thorough checks for lab-induced irreversible magnetic behavior that can skew paleointensity estimates. In the meantime, it is intriguing that some other analyses have already suggested that the intensity of the time-averaged GMF was considerably lower than the present-day value (Selkin and Tauxe, 2000; Yamamoto and Tsunakawa, 2005; Lawrence et al., 2009).

Acknowledgements

The 1993 field sampling was funded by INSU and organized by Hélène Collombat, with authorization of the National Park of the Galapagos Islands. We are grateful to Hélène Collombat and Pablo Samaniego for their essential contribution in the field work. This phase of laboratory work on the Galapagos samples was supported by NSF grant EAR0609339 (DVK). We thank the journal reviewers for helpful comments and Lisa Tauxe for ongoing discussions about paleosecular variation. Lamont-Doherty Earth Observatory contribution #7398.

References

Aitken, M.J., Allsop, A.L., Bussell, G.D., Winter, M.B., 1988. Determination of the intensity of the earth's magnetic field during archealogical times – reliability of the Thellier technique. Reviews of Geophysics 26, 3–12.

Bailey, K., 1976. Potassium–argon ages from the Galapagos Islands. Science 192, 465–467.

Coe, R.S., 1967. The determination of paleo-intensities of the earth's magnetic field with emphasis on mechanisms which could cause non-ideal behavior in Thellier's method. Journal of Geomagnetism and Geoelectricity 19 (3), 157–179.

Constable, C.G., Parker, R.L., 1988. Statistics of the geomagnetic secular variation for the past 5 m.y. Journal of Geophysical Research 93, 11569–11581.

Cox, A., 1962. Analysis of present geomagnetic field for comparison with paleomagnetic results. Journal of Geomagnetism and Geoelectricity 13, 101–112.

Cox, A., 1969. Confidence limits for the precision parameter *k*. Geophysical Journal of the Royal Astronomical Society 18, 545–549.

Cox, A., 1970. Latitude dependence of the angular dispersion of the geomagnetic field. Geophysical Journal of the Royal Astronomical Society 20, 253–269.

Cox, A., 1971. Paleomagnetism of San Cristobal Island, Galapagos. Earth and Planetary Science Letters 11, 152–160.

Cox, A., Dalrymple, G.B., 1966. Paleomagnetism and potassium-argon ages of some volcanic rocks from the Galapagos Islands. Nature 209, 776–777.

Creer, K.M., 1962. The dispersion of the geomagnetic field due to secular variation and its determination for remote times from paleomagnetic data. Journal of Geophysical Research 67, 3461–3476.

Creer, K.M., Irving, E., Nairn, A.E.M., 1959. Palaeomagnetism of the Great Whin Sill. Geophysical Journal of the Royal Astronomical Society 2, 306–323.

Day, R., Fuller, M., Schmidt, V.A., 1977. Hysteresis properties of titanomagnetites: grain-size and compositional dependence. Physics of the Earth and Planetary Interiors 13, 260–267.

Doell, R.R., Cox, A., 1971. Pacific geomagnetic secular variation. Science 171 (3968), 248–254.

Dunlop, D.J., Ozdemir, O., 2007. Magnetizations of rocks and minerals. In: Kono, M. (Ed.), Treatise on Geophysics. Elsevier, Amsterdam, pp. 277–336.

Elmaleh, A., Valet, J.P., Quidelleur, X., Solihin, A., Bouquerel, H., Tesson, T., Mulyadi, E., Khokhlov, A., Wirakusumah, A.D., 2004. Palaeosecular variation in Java and Bawean Islands (Indonesia) during the Brunhes chron. Geophysical Journal International 157, 441–454.

Herrero-Bervera, E., Valet, J.-P., 2009. Testing determinations of absolute paleointensity from the 1955 and 1960 Hawaiian flows. Earth and Planetary Science Letters 287 (3–4), 420–433.

Irving, E., Ward, M.A., 1964. A statistical model of the geomagnetic field. Geofisica pura e applicata (Pure and Applied Geophysics) 57, 47–52.

Jackson, A., Jonkers, A.R.T., Walker, M.R., 2000. Four centuries of geomagnetic secular variation from historical records. Philosophical Transactions of the Royal Society London A358, 957–990.

Johnson, C.L., Constable, C.G., Tauxe, L., Barendregt, R., Brown, L.L., Coe, R.S., Layer, P., Mejia, V., Opdyke, N.D., Singer, B.S., Staudigel, H., Stone, D.B., 2008. Recent investigations of the 0–5 Ma geomagnetic field recorded by lava flows. Geochemistry, Geophysics, Geosystems 9, Q04032, doi:10.1029/2007GC001696.

Kidane, T., Courtillot, V., Manighetti, I., Audin, L., Lahitte, P., Quidelleur, X., Gillot, P.-Y., Gallet, Y., Carlut, J., Haile, T., 2003. New paleomagnetic and geochronologic results from Ethiopian Afar: block rotations linked to rift overlap ad propagation and determination of a ~2 Ma reference pole for stable Africa. Journal of Geophysical Research 108, 2102, doi:10.1029/2001JB000645.

Kirschvink, J.L., 1980. The least-squares line and plane and the analysis of palaeomagnetic data. Geophysical Journal of the Royal Astronomical Society 62, 699–718.

Lawrence, K.P., Tauxe, L., Staudigel, H., Constable, C., Koppers, A., McIntosh, W., Johnson, C.L., 2009. Paleomagnetic field properties at high southern latitude. Geochemistry, Geophysics, Geosystems 10, Q01005, doi:10.1029/2008GC002072.

McBirney, A.R., 1994. Differentiated rocks of the Galapagos hotspot. Journal Geological Society of London.

McBirney, A.R., Williams, H., 1969. Geology and petrology of the Galapagos Islands. Geological Society of America Memoir 118, 1–197.

McElhinny, M.W., McFadden, P.L., 1997. Paleosecular variation over the past 5 Myr based on a new generalized database. Geophysical Journal International 131, 240–252.

McElhinny, M.W., Merrill, R.T., 1975. Geomagnetic secular variation over the past 5 m.y. Reviews of Geophysics and Space Physics 13, 687–708.

McFadden, P.L., McElhinny, M.W., 1990. Classification of the reversal test in palaeomagnetism. Geophysical Journal International 103, 725–729.

McFadden, P.L., Merrill, R.T., McElhinny, M.W., 1988. Dipole/quadrupole family modeling of paleosecular variation. Journal of Geophysical Research 93, 11583–11588.

Opdyke, N.D., Hall, M., Mejia, V., Huang, K., Foster, D.A., 2006. The time averaged field at the equator: results from Ecuador. Geochemistry, Geophysics, Geosystems 7, Q11005, doi:10.1029/2005GC001221.

Opdyke, N.D., Kent, D.V., Huang, K., Foster, D.A., Patel, J.P., 2010. Equatorial paleomagnetic time averaged field results from 0–5 Ma lavas from Kenya and the latitudinal variation of angular dispersion. Geochemistry, Geophysics, Geosystems 11, Q05005, doi:10.1029/2009GC002863.

Rochette, P., Ben Atig, F., Collombat, H., Vandamme, D., Vlag, P., 1997. Low paleosecular variation at the equator: a paleomagnetic pilgrimage from Galapagos to Esterel with Allan Cox and Hans Zijderveld. Geologie en Mijnbouw 76, 9–19.

Selkin, P.A., Tauxe, L., 2000. Long-term variations in paleointensity. Philosophical Transactions of the Royal Society of London A358, 1065–1088.

Short, P., 2000. Gilbert's De Magnete: an early study of magnetism and electricity. EOS 81, 233–234.

Sinton, C.W., Christie, D.M., Duncan, R.A., 1996. Geochronology of Galapagos seamounts. Journal of Geophysical Research 101, 13659–13700.

Swanson, F.J., Baitis, H.W., Lexa, J., Dymond, J., 1974. Geology of Santiago, Rabida and Pinzon Islands, Galapagos. Geological Society of America Bulletin 85, 1803–1810.

Tauxe, L., Kent, D.V., 2004. A simplified statistical model for the geomagnetic field and the detection of shallow bias in paleomagnetic inclinations: was the ancient magnetic field dipolar? In: Kono, M., Channell, J.E.T., Kent, D.V., Lowrie, W., Meert, J. (Eds.), Timescales of the Paleomagnetic Field, Geophysical Monograph 145. American Geophysical Union, Washington, DC, pp. 101–116.

Tauxe, L., Staudigel, H., 2004. Strength of the geomagnetic field in the cretaceous normal superchron: new data from submarine basaltic glass of the Troodos Ophiolite. Geochemistry, Geophysics, Geosystems 5, Q02H06, doi:10.1029/2003GC000635.

Thellier, E., Thellier, O., 1959. Sur l'intensité du champ magnétique terrestre dans le passé historique et géologique. Annales de Geophysique 15, 285–376.

Vandamme, D., 1994. A new method to determine paleosecular variation. Physics of the Earth and Planetary Interiors 85, 131–142.

White, W.M., McBirney, A.R., Duncan, R.A., 1993. Petrology and geochemistry of the Galapagos Islands: portrait of a pathological mantle plume. Journal of Geophysical Research 98, 19533–19563.

Wilson, R.L., 1971. Dipole offset – the time-averaged palaeomagnetic field over the past 25 million years. Geophysical Journal of the Royal Astronomical Society 22, 491–504.

Yamamoto, Y., Tsunakawa, H., 2005. Geomagnetic field intensity during the last 5 Myr: LTD-DHT Shaw palaeointensities from volcanic rocks of the Society Islands, French Polynesia. Geophysical Journal International 162, 79–114.